BIOLOGY
Methods & Protocols

OXFORD

Functional and comparative analysis of the Fe^{II}/2-oxoglutarate-dependent dioxygenases without using any substrate

Susmita Das[1], Nafeesa Shahnaz[1], Carmel Keerthana[1], Saumya Ranjan[1], Gayathri Seenivasan[1], Nikhil Tuti[1], Unnikrishnan P. Shaji[1], Gargi Meur[2] and Roy Anindya ![ORCID][1],*

[1]Department of Biotechnology, Indian Institute of Technology Hyderabad (IITH), Sanga Reddy, Kandi, Telangana 502284, India
[2]ICMR-National Institute of Nutrition, Hyderabad, Telangana 500007, India

*Corresponding author. Department of Biotechnology, Indian Institute of Technology Hyderabad (IITH), Sanga Reddy, Kandi, Telangana 502284, India.
E-mail: anindya@bt.iith.ac.in

Abstract

Non-haem iron (Fe^{II}) and 2-oxoglutarate(2OG)-dependent dioxygenases catalyse various biological reactions. These enzymes couple the oxidative decarboxylation of 2OG to the hydroxylation of the substrates. While some of these enzymes are reported to have multiple substrates, the substrate remains unknown for many of the enzymes. However, in the absence of the substrate, these enzymes catalyse oxidative decarboxylation of 2OG and generate succinate. We have determined succinate level to monitor this uncoupled reaction and compared the uncoupled 2OG turnover of different Fe^{II}/2OG-dependent dioxygenases. The uncoupled succinate production was used to verify the Ni^{II}-mediated inhibition and functionality of human dioxygenase ALKBH6.

Keywords: AlkB; DNA repair; uncoupled 2-oxoglutarate turnover; demethylation; Fe^{II}/2OG-dependent dioxygenase

Introduction

Iron and 2-oxoglutarate (2OG)-dependent dioxygenases (Fe^{II}/2OG dioxygenase) are involved in a variety of biochemical reactions, such as chromatin modification, fatty acid metabolism, regulating the hypoxic response, and repair of alkylated DNA[1]. These enzymes utilize non-haem ferrous iron (Fe^{II}) as a co-factor and 2OG as a co-substrate [2]. Oxidative decarboxylation of 2OG leads to the release of CO_2 and the formation of succinate [3]. The reaction catalysed by Fe^{II}/2OG-dependent dioxygenases consists of two half-reactions. The first half-reaction is O_2-activation leading to oxidative decarboxylation of 2OG to succinate and CO_2. The second half-reaction involves the transfer of the activated oxygen to the prime substrate, resulting in diverse outcomes such as desaturation, demethylations, ring-closure, and hydroxylation. These two half-reactions are generally coupled; however, sometimes decarboxylation of 2OG takes place even in the absence of any substrate. Such 2OG turnover is termed an uncoupled reaction and generally results in the oxidation of catalytic ferrous iron (Fe^{II}) which is subsequently reversed by ascorbic acid. The uncoupled reaction was described in many Fe^{II}/2OG-dependent dioxygenases, including prolyl hydroxylase, lysyl hydroxylase, and asparaginyl hydroxylase [4–6] and the AlkB family of nucleic acid demethylase [7], including ALKBH2, ALKBH3 [8], ALKBH5 [9], and ALKBH8 [10]. The rate of this uncoupled reaction was observed to be approximately 1%–5% of

the rate in the presence of substrate [11]. Due to distinct substrate specificity, it is not straightforward to compare the efficiency of Fe^{II}/2OG dioxygenases and we sought to examine if the comparative analysis of uncoupled 2OG turnover can be performed by determining the uncoupled activity. The Fe^{II}/2OG dioxygenase superfamily is extremely diverse and includes many enzymes without any known substrate. We were also interested to know whether the uncoupled conversion of 2OG to succinate can be used as a surrogate reaction to validate their functionality.

Most of the reports on the uncoupled activity of Fe^{II}/2OG-dependent dioxygenase involved the detection of the product released by adding ^{14}C-labelled 2OG and resulting ^{14}C-labelled succinate formation measured by scintillation counting [12]. Mass spectrometry-based methods for directly monitoring the product or the substrate were also applied [13, 14]. Although mass spectrometry or radiometric assay methods could detect picomolar level of succinate, these methods are technically challenging. Therefore, we used a colorimetric method for measuring uncoupled activity that employs *Escherichia coli* succinyl-CoA synthetase enzyme (SucCD) [15, 16]. In this report, we demonstrate the functionality of an AlkB family of Fe^{II}/2OG-dependent dioxygenase, the specific substrate of which remains unidentified. We also illustrate that succinate detection by this method is suitable for comparing the uncoupled activity of some well-characterized human Fe^{II}/2OG-dependent dioxygenases involved in DNA repair.

Materials and methods
Standard curve
A standard curve of phosphate was prepared using increasing concentrations of NaH_2PO_4 (0–200 μM) in 20 mM MES buffer, pH 6.5 and mixed with 100 μl of colorimetric solution (1:1 vol) consisting of vanadate-molybdate reagent. The mixture (200 μl) was incubated at room temperature for 5 min. Succinate standard curve was prepared by using increasing concentrations (0–200 μM) of succinate in buffer (20 mM MES buffer, pH 6.5). The colorimetric solution (100 μl) was added (1:1 vol) and the mixture (200 μl) was incubated at room temperature for 5 min. All the absorbance was recorded at 660 nm using a 96-well plate reader (Molecular Devices SpectraMax M5).

Cloning, expression and purification of recombinant E. coli SucCD protein
E. coli succinyl-CoA synthetase is a heterotetramer composed of *sucC* and *sucD* genes. The *sucC* gene encodes a polypeptide of 41.4 kDa that corresponds to the β subunit of succinyl-CoA synthetase. The *sucD* gene encodes a 29.7 kDa polypeptide, which constitutes the α subunit of succinyl-CoA synthetase. The sucC and sucD genes are translationally coupled as the stop codon present following the sucC gene overlaps with the sucD initiation codon by a single nucleotide [17]. Therefore, *sucC* and *sucD* genes were amplified by PCR using specific forward and reverse primers corresponding to sucC and sucD, respectively. The PCR amplified DNA was cloned between NdeI and XhoI of pET28a such that sucC and sucD proteins have N terminal and C terminal his-tag, respectively. The SDS-PAGE analysis of His-sucCD revealed two bands, one representing 43 kDa β-subunit (His-sucC) and the other band being 31 kDa α-subunit (His-sucD). The heteromeric protein was purified by using Ni-NTA agarose followed by gel-filtration chromatography.

Purification of recombinant Fe^{II}/2OG-dependent dioxygenase
Recombinant Fe^{II}/2OG-dependent dioxygenase, including AlkB, ALKBH2, ALKBH3, and Tpa1 were cloned as described before [18, 19]. Recombinant His-tag AlkBH6 was a generous gift from Prof Timothy O'Connor, City of Hope, Duarte Cancer Centre, USA. AlkB mutant (H131A, H133A), ALKBH2 mutant (H171A, D173A), ALKBH3 mutant (H191A, D193A, H257A), ALKBH6 mutant (H114A, D116A, H182A), Tpa1 mutant (H159C, D161N, H227C, H237C, R238A) were generated by site-directed mutagenesis. Wild type and mutant recombinant proteins were purified using standard Ni-affinity followed by gel filtration chromatography. Site-directed mutagenesis was used to generate the catalytic mutants of each enzyme as reported earlier [18, 19].

Succinate detection
The assay was performed in 96-well plate with 200 μl reaction volume. The succinate production by Fe^{II}/2OG dioxygenase (5-20 μM) were carried out in the buffer containing 20 mM Tris-HCl, pH 8.0, 2 mM ascorbate, 20 μM ammonium ferrous sulfate and 0.2 mM 2OG in final volume of 50 μl. The uncoupled reaction mixture was incubated up to 1 h at 37°C. The succinate formed in the reaction was detected by adding another 50 μl reaction mixture containing and Suc-CD enzyme (1 μM) in reaction buffer (20 mM MES, pH 6.5, 1 mM CoA, 1 mM ATP, 10 mM MgCl$_2$). The SucCD enzyme reaction was incubated for 1 h at 37°C. After incubation, 100 μl colorimetric solution (10% Ammonium molybdate in 10 N H_2SO_4 and 0.25 g of Ferrous sulphate in 5 ml water) was added to the reaction mixture (1:1, v/v) and incubated for 5 min. The absorbance was measured at 660 nm and the final succinate values were obtained from the succinate standard curve. The results were plotted and analysed using GraphPad Prism.

Time-dependent succinate detection
The time-dependent succinate production was measured by incubating dioxygenase enzyme (10 μM) in reaction buffer (50 μl) at 37°C. Part of the reaction mixture was removed every 20 min and stopped by adding 2 mM nickel chloride. Then sucCD was added and the reaction continued as mentioned above. The rate of the reaction was calculated from the slope of linear regression in GraphPad Prism.

Results and discussion
Comparative analysis of uncoupled succinate production of Fe^{II}/2OG-dependent dioxygenases
In the absence of substrate, active Fe^{II}/2OG-dependent dioxygenases decarboxylate the co-substrate 2OG to produce succinate and CO_2. Succinyl-CoA synthetase (SucCD) was used to determine succinate and with the concomitant hydrolysis of ATP to form ADP and phosphate. Using a molybdate reagent, the phosphate released was quantified colorimetrically [15] (Fig. 1A). We applied the same method for comparing the uncoupled succinate formation by four different Fe^{II}/2OG-dependent dioxygenases. Preparation of succinate standard revealed that lower limit of succinate detection using SucCD to be 0.2 μM (Fig. 1B). All the recombinant His-tag proteins were purified (Fig. 1C) as described before [18–22]. One of the important members of the Fe^{II}/2OG-dependent dioxygenase family is *E. coli* DNA repair enzyme AlkB [23], which catalyses the demethylation of 1meA and 3meC from DNA and RNA substrates. When the reaction was carried out in the presence of recombinant AlkB, 2OG, and ascorbate, but without any alkylated DNA substrate, the level of succinate production was determined (Fig. 1D). A highly conserved HX(D/E)X$_n$H triad motif supports acid residues responsible for Fe^{II}-binding and catalysis in all Fe^{II}/2OG dioxygenases [24]. To confirm that only catalytically active Fe^{II}/2OG dioxygenases can perform uncoupled 2OG turnover, we evaluated catalytically inactive mutant AlkB in the absence of substrate. As shown in Fig. 1D, this catalytically inactive AlkB did not show any uncoupled succinate production and suggested that this method could be reliably used to confirm uncoupled activity. Next, we evaluated *Saccharomyces cerevisiae* Fe^{II}/2OG dioxygenase Tpa1 and its catalytic mutant [19]. We confirmed the uncoupled succinate production from wild-type Tpa1 (Fig. 1E). We further examined two human AlkB homologues, ALKBH2 and ALKBH3. As a negative control, the succinate production of the catalytically dead ALKBH2 and ALKBH3 mutant were evaluated. As shown in Fig. 1F and G, ALKBH2 and ALKBH3 displayed uncoupled activity but not the catalytic mutants. We observed that some succinate is still produced in ALKBH mutants with all the catalytic triad residues removed. This could be due to hydrolysis of ATP by some undetected contaminant present in the mutant protein fractions.

Among the proteins examined, AlkB showed a saturation type succinate production with increasing concentration, unlike others. Presently, we do not know if this could be due to enzyme self-inactivation or some other mechanism. Taken together, these results suggest that succinate production could be used for determining uncoupled activity of Fe^{II} or 2OG binding in structure-function studies of this family of enzymes.
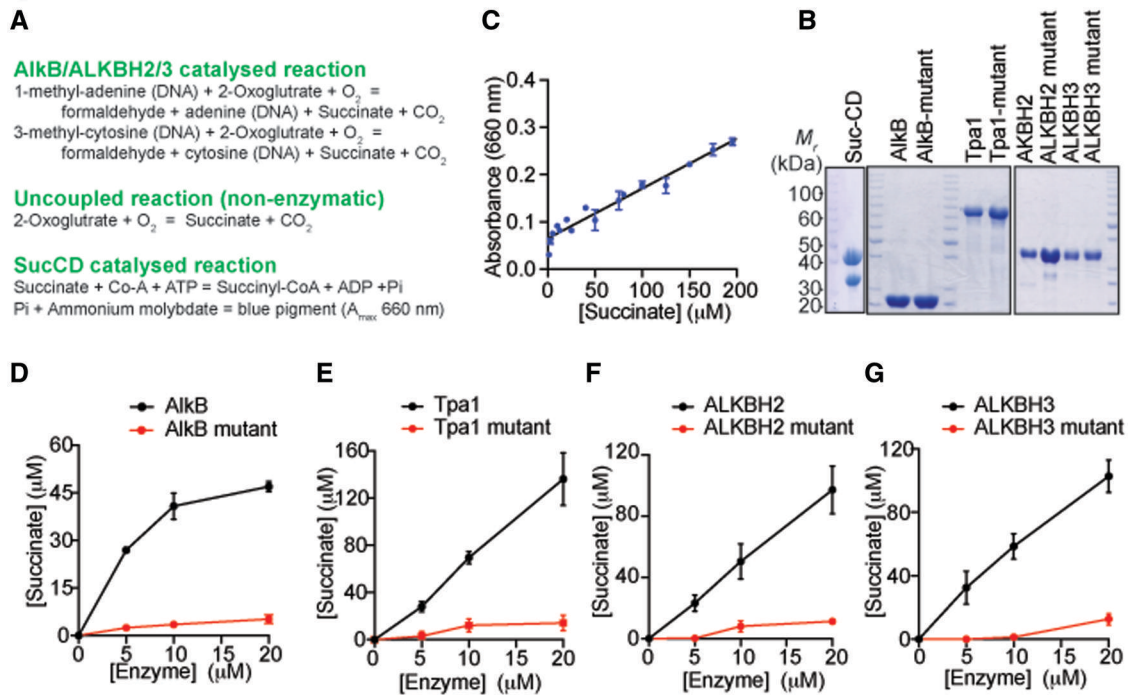
Figure 1 Comparative analysis of uncoupled succinate production by Fe^{II}/2OG-dependent dioxygenases. (**A**) Outline of reaction catalysed by Fe^{II}/2OG-dependent dioxygenases and SucCD enzymes and uncoupled reaction. (**B**) Standard graph of succinate for the range of 0.2–200 μM. (**C**) SDS-PAGE analysis of *E. coli* SucCD (75 kDa), wildtype and mutant AlkB (24 kDa), Tpa1 (77 kDa), ALKBH2 (33 kDa), and ALKBH3 (33 KDa). It should be noted that the protein loading is not equal for all proteins and differentially stained SDS-PAGE gels is depicted. (**D**) Enzyme concentration-dependent production of succinate monitored by the reaction of *E. coli* AlkB, (**E**) *S cerevisiae* TPA1, (**F**) ALKBH2, (**G**) ALKBH3. Error bar represent mean ± SE ($n = 4$)
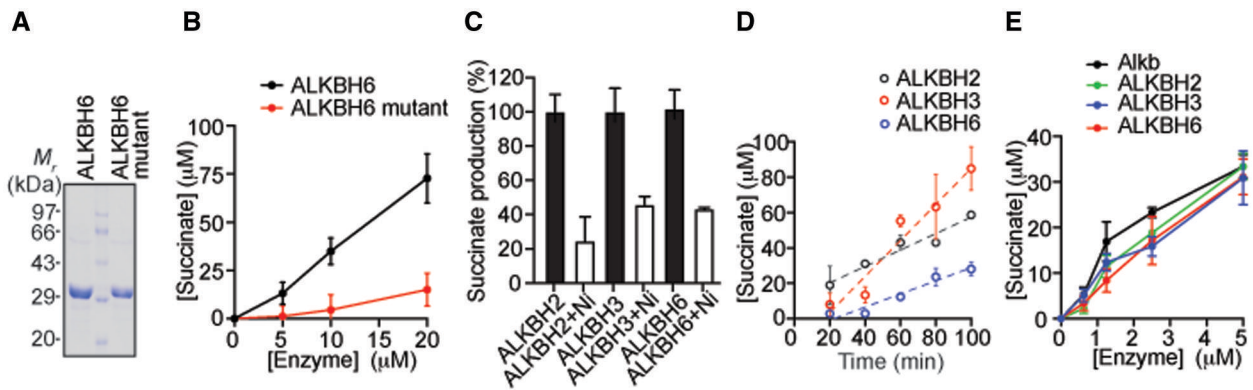
Figure 2 Production of uncoupled succinate by ALKBH6. (**A**) SDS-PAGE analysis of wildtype and mutant ALKBH6 (29 KDa). (**B**) Enzyme concentration-dependent production of succinate. (**C**) Inhibition of succinate production in the presence of nickel (Ni^{II}) ions. (**D**) Comparison of time-dependent increase of succinate production by ALKBH2, ALKBH3 and ALKBH6 (10 μM). Dashed lines represent the linear regression used for calculating the rate of succinate production. (**E**) Estimation of lower detection limit of succinate production by AlkB, ALKBH2, ALKBH3 and ALKBH6. Error bar represent mean ± SE ($n = 4$)

ALKBH6 is catalytically active Fe^{II}/2OG-dependent dioxygenase

Although many Fe^{II}/2OG-dependent dioxygenases are encoded in the human genome, it is not known whether they are all functional proteins. One such enzyme is the *E. coli* AlkB homologue ALKBH6. This enzyme was structurally and functionally characterized but the substrate of this enzyme is not known yet and biochemical activity could not be determined [25, 26]. We decided to verify the functionality of ALKBH6 using recombinant ALKBH6 and its catalytic mutant (Fig. 2A). When an increasing

concentration of ALKBH6 was incubated with the co-substrate 2OG without any substrate, succinate was produced in a dose-dependent manner (Fig. 2B). Previous studies reported that nickel (Ni^{II}) could replace the Fe^{II} in the catalytic centre of the Fe^{II}/2OG-dependent dioxygenases and cause inhibition of their enzymatic activity [27]. We monitored Ni^{II}-mediated inhibition of uncoupled 2OG turnover by adding nickel chloride to Fe^{II}-bound proteins. As expected, it reduced succinate production for all the enzymes tested (Fig. 2C). Interestingly, the magnitude of the inhibition varied between the enzymes. Whether this might be due to the

different affinities for the catalytic Fe^{II} among the enzymes could not be predicted as the binding affinity of Ni^{II} and Fe^{II} for any of the enzymes have not been reported.

Next, we measured time-dependent succinate production and derived the rate of uncoupled reaction (Fig. 2D). We observed that ALKBH3 showed highest rate of uncoupled succinate turnover ($1.02\,\mu M\,min^{-1}$) compared to ALKBH2 ($0.46\,\mu M\,min^{-1}$) and ALKBH6 ($0.37\,\mu M\,min^{-1}$). These results indicate that ALKBH6 is functionally active Fe^{II}/2OG-dependent dioxygenase and might display robust activity when the right substrate is identified. Finally we determined the lowest enzyme concentration that can be used in this method. Based on the standard graph of succinate, we could detect $0.5\,\mu M$ of AlkB, ALKBH2, ALKBH3, and ALKBH6 (Fig. 2E).

Conclusion

We demonstrated that the uncoupled succinate production could be used for comparing the uncoupled activity of the Fe^{II}/2OG-dependent dioxygenases and establishing the functionality of any Fe^{II}/2OG-dependent dioxygenases when the identity of the substrate is unknown. One limitation of this uncoupled succinate detection assay is that its detection limit is restricted to micromolar range. As the uncoupled reactions occur without any substrate, they do not follow Michalis–Menten reaction and as a result, it is not possible to determine Vmax and Km. However, this assay can be used for screening inhibitor without the need of substrate.

Author contributions

Susmita Das (Data curation [equal], Formal analysis [equal]), Nafeesa Shahnaz (Methodology [equal]), Carmel L. Keerthana (Data curation [equal], Formal analysis [equal]), Saumya Ranjan (Data curation [equal], Formal analysis [equal]), Gayathri Seenivasan (Data curation [equal], Formal analysis [equal]), Nikhil Tuti (Data curation [equal], Formal analysis [equal]), Unnikrishnan Shaji (Formal analysis [equal]), Gargi Meur (Conceptualization [equal], Funding acquisition [equal], Supervision [equal], Writing—review & editing [equal]), and Roy Anindya (Conceptualization [equal], Data curation [equal], Funding acquisition [equal], Methodology [equal], Resources [equal], Validation [equal], Writing—original draft [equal], Writing—review & editing [equal])

Conflict of interest statement. None declared.

Funding

References

1. Hausinger RP. FeII/alpha-ketoglutarate-dependent hydroxylases and related enzymes. *Crit Rev Biochem Mol Biol* 2004; **39**:21–68.
2. Martinez S, Hausinger RP. Catalytic mechanisms of Fe(II)- and 2-oxoglutarate-dependent oxygenases. *J Biol Chem* 2015; **290**:20702–11.
3. Herr CQ, Hausinger RP. Amazing diversity in biochemical roles of Fe(II)/2-oxoglutarate oxygenases. *Trends Biochem Sci* 2018; **43**:517–32.
4. Puistola U, Turpeenniemi-Hujanen TM, Myllylä R, Kivirikko KI. Studies on the lysyl hydroxylase reaction. II. Inhibition kinetics and the reaction mechanism. *Biochim Biophys Acta* 1980; **611**:51–60.
5. Tuderman L, Oikarinen A, Kivirikko KI. Tetramers and monomers of prolyl hydroxylase in isolated chick-embryo tendon cells. The association of inactive monomers to active tetramers and a preliminary characterization of the intracellular monomer-size protein. *Eur J Biochem* 1977;**78**:547–56.
6. Chen Y-H, Comeaux LM, Eyles SJ, Knapp MJ. Auto-hydroxylation of FIH-1: an Fe(II), alpha-ketoglutarate-dependent human hypoxia sensor. *Chem Commun* 2008;4768–70.
7. Henshaw TF, Feig M, Hausinger RP. Aberrant activity of the DNA repair enzyme AlkB. *J Inorg Biochem* 2004;**98**:856–61.
8. Monsen VT, Sundheim O, Aas PA *et al.* Divergent ß-hairpins determine double-strand versus single-strand substrate recognition of human AlkB-homologues 2 and 3. *Nucleic Acids Res* 2010; **38**:6447–55.
9. Thalhammer A, Bencokova Z, Poole R *et al.* Human AlkB homologue 5 is a nuclear 2-oxoglutarate dependent oxygenase and a direct target of hypoxia-inducible factor 1α (HIF-1α). *PLoS One* 2011;**6**:e16210.
10. Jeltsch A, Zdżalik D, Vågbø CB *et al.* Protozoan ALKBH8 oxygenases display both DNA repair and tRNA modification activities. *PLoS ONE* 2014;**9**:e98729.
11. Myllylä R, Majamaa K, Günzler V *et al.* Ascorbate is consumed stoichiometrically in the uncoupled reactions catalyzed by prolyl 4-hydroxylase and lysyl hydroxylase. *J Biol Chem* 1984; **259**:5403–5.
12. Sabourin PJ, Bieber LL. Purification and characterization of an alpha-ketoisocaproate oxygenase of rat liver. *J Biol Chem* 1982; **257**:7460–7.
13. Bian K, Lenz SAP, Tang Q *et al.* DNA repair enzymes ALKBH2, ALKBH3, and AlkB oxidize 5-methylcytosine to 5-hydroxymethylcytosine, 5-formylcytosine and 5-carboxylcytosine in vitro. *Nucleic Acids Res* 2019;**47**:5522–9.
14. Whetstine JR, Nottke A, Lan F *et al.* Reversal of histone lysine trimethylation by the JMJD2 family of histone demethylases. *Cell* 2006;**125**:467–81.
15. Guo C, Hu Y, Yang C *et al.* Developing a colorimetric assay for Fe (II)/2-oxoglutarate-dependent dioxygenase. *Anal Biochem* 2018; **548**:109–14.
16. Luo L, Pappalardi MB, Tummino PJ *et al.* An assay for Fe(II)/2-oxoglutarate-dependent dioxygenases by enzyme-coupled detection of succinate formation. *Anal Biochem* 2006;**353**:69–74.
17. Buck D, Spencer ME, Guest JR. Primary structure of the succinyl-CoA synthetase of Escherichia coli. *Biochemistry* 1985; **24**:6245–52.
18. Mohan M, Akula D, Dhillon A *et al.* Human RAD51 paralogue RAD51C fosters repair of alkylated DNA by interacting with the ALKBH3 demethylase. *Nucleic Acids Res* 2019;**47**:11729–45.
19. Shivange G, Kodipelli N, Monisha M, Anindya R. A role for Saccharomyces cerevisiae Tpa1 protein in direct alkylation repair. *J Biol Chem* 2014;**289**:35939–52.
20. Deepa A, Naveena K, Anindya R. DNA repair activity of Fe(II)/2OG-dependent dioxygenases affected by low iron level in *Saccharomyces cerevisiae*. *FEMS Yeast Res* 2018;**18**:1–14.

21. Nigam R, Anindya R. Escherichia coli single-stranded DNA binding protein SSB promotes AlkB-mediated DNA dealkylation repair. *Biochem Biophys Res Commun* 2018;**496**:274–9.

22. Shivange G, Monisha M, Nigam R *et al.* RecA stimulates AlkB-mediated direct repair of DNA adducts. *Nucleic Acids Res* 2016;**44**:8754–63.

23. Sedgwick B, Bates PA, Paik J *et al.* Repair of alkylated DNA: recent advances. *DNA Repair (Amst)* 2007;**6**:429–42.

24. Loenarz C, Schofield CJ. Oxygenase catalyzed 5-methylcytosine hydroxylation. *Chem Biol* 2009;**16**:580–3.

25. Ma L, Lu H, Tian Z *et al.* Structural insights into the interactions and epigenetic functions of human nucleic acid repair protein ALKBH6. *J Biol Chem* 2022;**298**:101671.

26. Zhao S, Devega R, Francois A, Kidane D. ALKBH6 is required for maintenance of genomic stability and promoting cell survival during exposure of alkylating agents in pancreatic cancer. *Front Gen* 2021;**12**:635808.

27. Chen H, Costa M. Iron- and 2-oxoglutarate-dependent dioxygenases: an emerging group of molecular targets for nickel toxicity and carcinogenicity. *BioMetals* 2009;**22**:191–6.